Thermal attenuation in atom-surface scattering : the two phonon contribution

G. Armand(+), J. R. Manson (*) and C. S. Jayanthi (**)

(+) Service de physique des atomes et des surfaces, centre d'études nucléaires de Saclay, 91191 Gif-sur-Yvette Cedex, France

(*) Department of Physics and Astronomy, Clemson University, Clemson, SC 29631, U.S.A.

Résumé. — L'intensité du faisceau spéculaire produit par la diffusion d'un faisceau de particules incidentes mono-énergétiques par une surface plane, est calculée en fonction de la température du cristal. Le calcul inclut les processus virtuels à un et deux phonons. La procédure exposée précédemment [1, 2] est utilisée et permet de calculer exactement les éléments de matrice des sept différents diagrammes décrivant les échanges virtuels de deux phonons. Pour tous les systèmes étudiés (He-Cu, H_2-Cu, Ne-Cu) les résultats indiquent que la contribution la plus importante à l'intensité est donnée par les diagrammes provenant de l'ordre le plus élevé dans le développement en perturbation. L'intensité totale est plus grande que celle donnée par le processus à 1 phonon seul, excepté à très basse température. La température à partir de laquelle la contribution des effets de deux phonons devient appréciable est en général basse. Les intensités calculées reproduisent les données expérimentales dans le domaine de température ou les contributions des processus à 3 phonons ou plus sont négligeables.

Abstract. — The specular intensity produced by the scattering of monoenergetic incident particles by a flat surface is calculated as a function of the crystal temperature including one and two virtual phonon processes. The exact procedure developed previously [1, 2] is employed in order to get the matrix elements of the seven different two phonon diagrams. For all the different systems studied (He-Cu, H_2-Cu, Ne-Cu) the results show that the most efficient two-phonon term is the diagram of highest order in the perturbation expansion. The total intensity is greater than that obtained by considering the one phonon process alone except at very low crystal temperature. The temperature for which the two phonon contribution becomes non-negligible is in general low. Comparison with available experimental data gives good agreement in the temperature domain where higher order phonon processes could be neglected.

1. Introduction.

To date many papers have been published dealing with elastic diffraction studies of monoenergetic particle beams scattered by ordered surfaces. The general purpose of these works is the determination of the interaction potential particle surface, either by theoretical calculation from first principles or by construction of a potential model. If some important progress has been made in this direction many problems remain to be solved. One of the most important and perharps difficult is certainly to relate the thermal crystal agitation to the thermal fluctuation of the interaction potential.

As a contribution to the solution of this problem we have developed recently a procedure which allows us to calculate exactly the diffraction peak intensities or the cross section of inelastic events as a function of the crystal temperature [1, 2]. Up to now this procedure has been used to calculate the effect of the one phonon virtual process on the specular intensity of a helium particle scattered by a flat surface. The atomic crystal vibration is introduced through either harmonic [1, 2] or quasi-harmonic approximation [3].

In this paper we extend the above calculation in order to include the effects of the seven different diagrams which describe the totality of the two phonon virtual processes. Results are presented in the case where experimental data are available, that is to say for the scattering of helium, molecular hydrogen and neon by the (100) copper face. With these particles the different parameters such as their mass, potential

(**) *Present address* : Max-Planck Institüt für Festkörper-forschung — Heisenbergstrasse 1 — D-7000, Stuttgart-80, F.R.G.

well depth and damping coefficient, vary in a sufficiently large domain. Thus their influence on the elastic intensity can be evaluated.

2. General theory.

In inelastic scattering theory the transition rate $_f w_i$ between initial (i) and final (f) states is proportional to the square modulus of the T matrix element :

$$_f w_i \simeq |_f T_i|^2 .$$

By performing on this expression the usual Van Hove transformation one gets the reflection coefficient :

$$_f R_i \simeq \int_{-\infty}^{+\infty} dt \exp\left[i \frac{t}{\hbar}(E_f - E_i) \right] \langle\langle _f T_i^+ (t=0) \, _f T_i(t) \rangle\rangle$$

$$(1)$$

where E_f and E_i are respectively the final and initial energy of the scattered particle, and where the double bracket $\langle\langle \ \rangle\rangle$ stands for a thermal average over crystal phonon states.

If the final particle state coincides with a diffracted beam Levi and Suhl [4] have shown that expression (1) is greatly simplified and reduces to

$$_G R_i \simeq |\langle\langle _G T_i \rangle\rangle|^2 . \qquad (2)$$

This can be understood in the following way. The thermal average in (1) yields time dependent correlation functions between crystal atom displacements. This expression can be expanded in powers of the correlated displacement and the zero order term, that is to say the time independent term, gives the elastic contribution. This can be calculated directly by performing the thermal average of

$$\langle\langle _f T_i^+ (t = 0) \, _f T_i(t = 0) \rangle\rangle$$

which is equal to $|\langle\langle _f T_i \rangle\rangle|^2$, and expression (2) is recovered.

Throughout this paper we intend to calculate the two phonon contribution to the thermal attenuation of the specular beam. Thus it is sufficient to obtain the thermal average of the T matrix element $_i T_i$, including one and two phonon processes.

The simple procedure which allows one to calculate this average exactly has been presented in some preceding papers [1, 2], for the general case of a corrugated surface. Therefore we just give here a brief account of this procedure.

Let us consider the T matrix equation :

$$T = V(\mathbf{R}, z, \mathbf{u}) - U(z) + (V(\mathbf{R}, z, \mathbf{u}) - U'(z)) G^+ T \quad (3)$$

where V is the potential depending upon space coordinate through $\mathbf{R}$ and z (which are components respectively parallel and normal to the surface), and crystal thermal atom motion denoted by the symbolic operator $\mathbf{u}$. G^+ is the Green operator for the problem at hand :

$$G^+ = (c + E_i^{(c)} - H^{(c)} + i\varepsilon)^{-1}, \quad c = E_i - H_0,$$

$$H_0 = -\frac{\hbar^2}{2m}\nabla^2 + U(z)$$

in which $E_i^{(c)}$ and $H^{(c)}$ are respectively the initial energy and harmonic Hamiltonian of the crystal. H_0 the Hamiltonian of the distorted potential $U(z)$, and m the mass of the incident particle.

Taking an integral representation of G^+ namely

$$G^+ = -\frac{i}{\hbar} \int_0^\infty \exp\left[i(c + E_i^{(c)} - H^{(c)} + i\varepsilon)\frac{t}{\hbar} \right] dt$$

equation (3) can be written as :

$$T = V - U - \frac{i}{\hbar} \int_0^\infty \exp\left(iE_i^{(c)}\frac{t}{\hbar} \right)(V - U) \times$$

$$\times \exp\left(i(c - H^{(c)} + i\varepsilon)\frac{t}{\hbar} \right) T \, dt .$$

Then inserting on the left of $V - U$ the factor

$$\exp\left(-iH^{(c)}\frac{t}{\hbar} \right)\exp\left(iH^{(c)}\frac{t}{\hbar} \right) = 1$$

one gets :

$$T = V - U - \frac{i}{\hbar} \int_0^\infty \exp\left(i(E_i^{(c)} - H^{(c)})\frac{t}{\hbar} \right)(V(\mathbf{u}(t)) - U(z)) \exp\left(i(c + i\varepsilon)\frac{t}{\hbar} \right) T \, dt$$

$V(\mathbf{u}(t))$ is now the potential $V(\mathbf{R}, z, \mathbf{u})$ in the interaction picture. In the calculation of the T matrix element between crystal state $|n_i\rangle$ corresponding to the energy $E_i^{(c)}$, the first exponential under the integral is unity and the thermal average is given by :

$$\langle\langle _i T_i \rangle\rangle = \langle\langle V(\mathbf{R}, z, \mathbf{u}) - U(z) \rangle\rangle - \frac{i}{\hbar} \int_0^\infty \left\langle\left\langle (V(\mathbf{R}, z, \mathbf{u}(t)) - U(z)) \exp\left(i(c + i\varepsilon)\frac{t}{\hbar} \right) T \right\rangle\right\rangle dt . \quad (4)$$

The iteration of this equation gives the perturbation expansion. One gets with $v(u) = V(\mathbf{R}, z, \mathbf{u}) - U(z)$:

$$\langle\!\langle\, _iT_i\,\rangle\!\rangle = \langle\!\langle\, v(\mathbf{u})\,\rangle\!\rangle - \frac{i}{\hbar}\int_0^\infty dt\,\Big\langle\!\Big\langle\, v(\mathbf{u}(t))\exp\!\Big((ic - \varepsilon)\frac{t}{\hbar}\Big)v(\mathbf{u})\,\Big\rangle\!\Big\rangle +$$

$$+ \Big(-\frac{i}{\hbar}\Big)^2\iint_0^\infty dt_1\,dt_2\,\Big\langle\!\Big\langle\, v(\mathbf{u}(t_1 + t_2))\exp\!\Big((ic - \varepsilon)\frac{t_2}{\hbar}\Big)v(\mathbf{u}(t_1))\exp\!\Big((ic - \varepsilon)\frac{t_1}{\hbar}\Big)v(\mathbf{u})\,\Big\rangle\!\Big\rangle$$

$$+ \Big(-\frac{i}{\hbar}\Big)^3\iiint_0^\infty dt_1\,dt_2\,dt_3\,\Big\langle\!\Big\langle\, v(\mathbf{u}(t_1 + t_2 + t_3))\exp\!\Big((ic - \varepsilon)\frac{t_3}{\hbar}\Big)v(\mathbf{u}(t_1 + t_2))$$

$$\times \exp\!\Big((ic - \varepsilon)\frac{t_2}{\hbar}\Big)v(\mathbf{u}(t_1))\exp\!\Big((ic - \varepsilon)\frac{t_1}{\hbar}\Big)v(\mathbf{u})\,\Big\rangle\!\Big\rangle$$

$$+ \cdots . \tag{5}$$

In each term the remaining exponentials depend upon particle coordinates only through c. One can carry out the thermal average and then the integration on the t variables. In this way all orders of expansion could be calculated exactly.

3. Flat surface.

As in preceding papers [1, 2] we consider the scattering of a neutral particle by a flat surface. The particle surface interaction is modeled by a soft potential :

$$V = D[\exp(-2\chi(z - u) - 2\chi^2\langle\!\langle\, u^2\,\rangle\!\rangle) - f(z)] . \tag{6}$$

Its attractive part is stationary while its repulsive part is thermally displaced in the direction normal to the surface through the displacement operator u. This last quantity should be suitably chosen, in order to reproduce as well as possible the influence of crystal atom motion on the potential.

For such a choice of the model potential the particle can gain or lose energy without any change of its momentum component parallel to the surface. The following calculation is therefore the quantum mechanical equivalent of the old one dimensional classical inelastic theories, in which one supposes the conservation of the parallel component of the incident particle speed.

Due to the lack of parallel momentum exchange the description of physical reality is not complete. Nevertheless the results should reproduce the general evolution of the thermal attenuation with respect to the number of phonons taken into account, and with respect to the different potential parameters. Particularly, the effect of assisted resonance with bound states by phonons exchange is exactly included in the calculation.

The thermal average of (6) is

$$\langle\!\langle\, V\,\rangle\!\rangle = D(\exp(-2\chi z) - f(z)) .$$

In the following we make the choice $U(z) = \langle\!\langle\, V\,\rangle\!\rangle$, and consequently :

$$v(u) = D\exp(-2\chi z)(\exp(2\chi u - 2\chi^2\langle\, u^2\,\rangle) - 1) . \tag{7}$$

Obviously $\langle\!\langle\, v(\mathbf{u})\,\rangle\!\rangle = 0$, and the first order term in the perturbation expansion (5) does not contribute to the averaged T matrix element.

Note that the eigenvalues and eigenstates of the distorted potential will be denoted by e and ϕ respectively. The subscript p and b on these quantities label respectively continuum and bound states. As in previous papers we use dimensionless quantities defined with the help of the inverse energy factor $A^2 = 2m/\hbar^2\,\chi^2$. They become :

frequency
energy
time

$$_iT_i \to {}_iF_i = 4A^2\,_iT_i$$
$$\omega \to \Omega = A^2\,\hbar\omega$$
$$\begin{cases} e_p \to p^2 = A^2\,e_p \\ e_b \to \Omega_b = A^2\,|e_b| \end{cases}$$
$$t \to \tau = \frac{t}{\hbar A^2} .$$

In terms of these dimensionless quantities the reflection coefficient to be calculated is given by

$$_iR_i = |1 - i\pi\,_iF_i/4p_i|^2 . \tag{8}$$

4. Second order term.

With $v(u)$ given by expression (7) the thermal average can be made easily and the second term in expansion (5) becomes :

$$\langle\!\langle\, _iT_i^{(2)}\,\rangle\!\rangle = -\frac{i}{\hbar}D^2\Big\langle\, e^{i\mathbf{K}_i\cdot\mathbf{R}}\,\phi_i\,\Big|\int_0^\infty dt\exp(-2\chi z)\exp\!\Big((ic - \varepsilon)\frac{t}{\hbar}\Big)(W(t, 0) - 1)\exp(-2\chi z)\Big|\,\phi_i\,e^{i\mathbf{K}_i\cdot\mathbf{R}}\,\Big\rangle$$

with $|\mathbf{K}_i| = k_i \sin\theta_i$, k_i the incident wavevector, θ_i the incident angle, and

$$W(t, 0) = \exp(4\,\chi^2 \langle\!\langle u(t)\,u(0) \rangle\!\rangle)\,.$$

The correlation function is given by :

$$\langle\!\langle u(t)\,u(0) \rangle\!\rangle = \frac{\hbar}{2M} \int_0^{\omega_m} \frac{\rho(\omega)}{\omega}[(\langle\!\langle n(\omega) \rangle\!\rangle + 1)\exp(-i\omega t) + \langle\!\langle n(\omega) \rangle\!\rangle \exp(i\omega t)]\,d\omega$$

where $\langle\!\langle n(\omega) \rangle\!\rangle$ is the Bose-Einstein factor, $\rho(\omega)$ the spectral density of u and M the mass of a crystal atom. Noting that $\langle\!\langle n(\omega) \rangle\!\rangle + 1 = -\langle\!\langle n(\omega) \rangle\!\rangle$ and putting $\rho(-\omega) = \rho(\omega)$ this expression is transformed into :

$$\langle\!\langle u(t)\,u(0) \rangle\!\rangle = \frac{\hbar}{2M} \int_{-\omega_m}^{+\omega_m} \frac{\rho(\omega)}{\omega} \langle\!\langle n(\omega) \rangle\!\rangle \exp(i\omega t)\,d\omega$$

which in dimensionless form becomes

$$4\,\chi^2 \langle\!\langle u(t)\,u(0) \rangle\!\rangle = 4\frac{m}{M} \int_{-\Omega_m}^{+\Omega_m} \frac{\rho(\Omega)}{\Omega} \langle\!\langle n(\Omega) \rangle\!\rangle \exp(i\Omega\tau)\,d\Omega\,. \tag{9}$$

Now we expand $W(T, 0)$ in powers of the correlation function and consider for the moment the first order term (for order 0 it gives 1). The integration over t yields a modified Green operator which depicts an exchange of one phonon :

$$G^+(\omega) = (E_i - H_0 + \hbar\omega + i\varepsilon)^{-1}\,.$$

This dressed propagator is located between two $\exp(-2\chi z)$ factors. The introduction of the projector states in $\langle\!\langle _i T_i^{(2)} \rangle\!\rangle$ yields, after transformation into dimensionless quantities :

$$_iF_i^{(2,1)} = 4(A^2 D)^2 \frac{4m}{M} \int_{-\Omega_m}^{+\Omega_m} d\Omega\, \frac{\rho(\Omega)}{\Omega} \langle\!\langle n(\Omega) \rangle\!\rangle \times \int_0^x \left[\frac{_p f_p\, _p f_{p_i}\, dp}{p_i^2 - p^2 + \Omega + i\varepsilon} + \sum_b \frac{_{p_i} l_b\, _b l_{p_i}}{p_i^2 + \Omega_b + \Omega + i\varepsilon} \right] \tag{10}$$

with

$$p_i^2 = (k_i^2 - |\mathbf{K}_i|^2)\chi^{-2}, \quad _p f_p = \langle \phi_{p_i} | \exp(-2\chi z) | \phi_p \rangle, \quad _{p_i} l_b = \langle \phi_{p_i} | \exp(-2\chi z) | \phi_b \rangle\,.$$

The physical interpretation of this equation is straightforward, noting that $p_i^2 + \Omega$ is the normal kinetic energy of a particle which has gained ($\Omega > 0$) or lost ($\Omega < 0$) the phonon energy corresponding to Ω. The expression in brackets is the matrix element of a particle scattered elastically by the thermally averaged potential but having a normal energy $p_i^2 + \Omega$ during the propagation between the initial and final states. On the other hand one can say that the particle goes from an initial state to continuum (p) or bound (b) state with the matrix element $_p f_{p_i}$ or $_b l_{p_i}$ and with creation or a annihilation of one phonon. It propagates and undergoes the reverse process in order to go out into the final state which is identical to the initial one.

During the propagation the particle energy is not conserved except for Ω values which cause the denominators to vanish. These occurrences are given respectively by the principal value integral and the delta function yielded by the Green operator. The occurrence of transitory non-energy conservation processes, which is a purely quantum effect, should be kept in mind when results are compared with those of a semi-classical theory.

It is important also to notice that the resonances assisted by phonon exchange are correctly included in the calculation.

The whole one phonon process is depicted diagrammatically in figure 1a : the vertex represents the matrix elements and the lines the dressed Green operator. It is assumed that the integration over all frequencies has been carried out, the matrix element being multiplied by the weighting factor given in expression (10).

In order to have a simpler representation of the following two phonon expressions it is more convenient to perform the integration over Ω prior to those over p. This gives :

$$_iF_i^{(2,1)} = 4(A^2 D)^2 \left[\int_0^x {}_p f_p\, G^{(2,1)}(C_p, T)\, _p f_{p_i}\, dp + \sum_b {}_{p_i} l_b\, G^{(2,1)}(C_b, T)\, _b l_{p_i} \right], \tag{11}$$
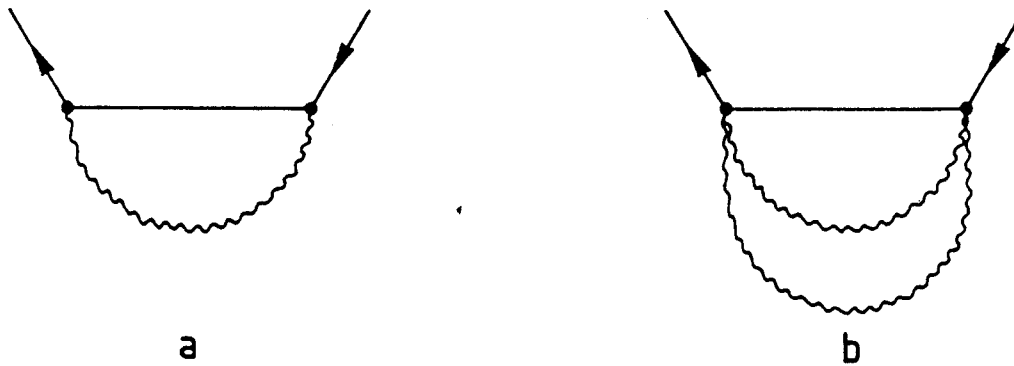
Fig. 1. — Second order diagrams — a) one virtual phonon process, b) two virtual phonon process.

with

$$G^{(2,1)}\left\{\begin{matrix}(C_p, T)\\(C_b, T)\end{matrix}\right\} = \frac{4\,m}{M}\int_{-\Omega_m}^{+\Omega_m}\frac{\rho(\Omega)}{\Omega}\ll n(\Omega)\gg\frac{d\Omega}{\left\{\begin{matrix}C_p\\C_b\end{matrix}\right\}+\Omega+i\varepsilon}$$ (12)

and $C_p = p_i^2 - p^2$, $C_b = p_i^2 + \Omega_b$, where T labels the crystal temperature.

The second order term in the $W(t, 0)$ expansion is equal to :

$$\frac{1}{2!}(4\,\chi^2\ll u(t)\,u\gg)^2 .$$

Expression (9) shows that its contribution to the t integration is

$$\exp(i(\Omega + \Omega')\,\tau)$$

and the modified Green function is therefore :

$$G^+(\omega + \omega') = [E_i - H_0 + \hbar(\omega + \omega') + i\varepsilon]^{-1} .$$

This clearly yields a two phonon exchange. The preceding interpretation is valid and the corresponding diagram is represented in figure 1b. The dimensionless $\ll T \gg$ matrix element is given by

$$_iF_i^{(2,2)} = \frac{4}{2!}(A^2\,D)^2\left[\int_0^\infty {}_{p}f_{p}\,G^{(2,2)}(C_p, T)\,{}_{p}f_{p_i}\,dp + \sum_b {}_{p_i}l_b\,G^{(2,2)}(C_b, T)\,{}_bl_{p_i}\right]$$ (13)

with :

$$G^{(2,2)}\left\{\begin{matrix}C_p, T\\C_b, T\end{matrix}\right\} = \frac{4\,m}{M}\int_{-\Omega_m}^{+\Omega_m}\frac{\rho(\Omega)}{\Omega}\ll n(\Omega)\gg G^{(2,1)}\left\{\begin{matrix}C_p + \Omega, T\\C_b + \Omega, T\end{matrix}\right\}d\Omega$$ (14)

where generally speaking

$$G^{(2,1)}(C + \Omega, T) = \frac{4\,m}{M}\int_{-\Omega_m}^{+\Omega_m}\frac{\rho(\Omega')}{\Omega'}\ll n(\Omega')\gg\frac{d\Omega'}{C + \Omega + \Omega' + i\varepsilon}$$ (15)

$G^{(2,2)}$ is therefore proportional to $\left(\dfrac{m}{M}\right)^2$.

The following higher order terms in the $W(t)$ expansion will give three, four and further multiple phonon exchange. Each term is composed of two matrix elements (vertices) and one dressed Green propagator. The corresponding $\ll T \gg$ matrix element will be given by an expression similar to (11) or (13) with the appropriate G function. For the n phonon exchange $G^{(2,n)}$ contains n integrations over Ω and therefore it will be proportional to $\dfrac{1}{n!}\left(\dfrac{m}{M}\right)^n$. One can expect this yields negligeable $\ll T \gg$ matrix elements except in the case where the mass ratio m/M is close to or higher than 1, or if the matrix elements f and l are large, that is to say for very high χ values.

5. Third order term.

After evaluating the thermal average the third term in expression (5) can be written as :

$$\langle\!\langle {}_iT_i^{(3)}\rangle\!\rangle = \left(-\frac{i}{\hbar}\right)^2 D^3 \left\langle e^{i\mathbf{K}_i\cdot\mathbf{R}}\,\phi_i \left| \int_0^x \int_0^x dt_2\,dt_1 \exp(-2\,\chi z)\times \right.\right.$$

$$\left.\left.\times \exp\!\left((ic-\varepsilon)\frac{t_2}{\hbar}\right)\exp(-2\,\chi z)\exp\!\left((ic-\varepsilon)\frac{t_1}{\hbar}\right)\exp(-2\,\chi z)\,W(t_2,t_1)\right| e^{i\mathbf{K}_i\cdot\mathbf{R}}\,\phi_i\right\rangle.$$

Noting that $W(t_1+t_2,t_1)=W(t_2,0)$, one has :

$$W(t_2,t_1) = [W(t_2,0)\,W(t_1+t_2,0)\,W(t_1,0)-1]-[W(t_2,0)-1]-[W(t_1+t_2,0)-1]-[W(t_1,0)-1].$$

With a little algebra this expression is transformed into :

$$W(t_2,t_1) = [W(t_2,0)-1][W(t_1,0)-1]+[W(t_2,0)\,W(t_1,0)-1]\times[W(t_1+t_2,0)-1].$$

The expansion of the different W functions up to first order leads to :

$$W(t_2,t_1) = 4\,\chi^2\langle\!\langle u(t_2)\,u\rangle\!\rangle\,4\,\chi^2\langle\!\langle u(t_1)\,u\rangle\!\rangle + 4\,\chi^2(\langle\!\langle u(t_2)\,u\rangle\!\rangle + \langle\!\langle u(t_1)\,u\rangle\!\rangle)\,4\,\chi^2\langle\!\langle u(t_1+t_2)\,u\rangle\!\rangle.$$

The contributions of these terms to the t_2 and t_1 integrations are respectively :

$$\exp i(\Omega_2\,\tau_2+\Omega_1\,\tau_1),\quad [\exp(i\Omega_2\,\tau_2)+\exp(i\Omega_1\,\tau_1)]\exp(i\Omega(\tau_1+\tau_2))$$

which depict clearly a two phonon exchange. The integrations lead to two dressed Green operators located between the three factors $\exp(-2\,\chi z)$. The diagrammatic representation is given in figure 2a and 2b respectively for the first and second term. The latter yields two diagrams which are symmetric.

In order to calculate the corresponding $\langle\!\langle T\rangle\!\rangle$ matrix element one introduces two projectors. This yields four different terms describing the transition *via* continum-continum, bound-continum, continum-bound and bound-bound states. One gets :

— diagram 2a :

$$
{}_iF_i^{(3,2)} = 4(A^2 D)^3 \left\{
\begin{aligned}
&\iint_0^x {}_{p_i}f_p\,G^{(2,1)}(C_p,T)\,{}_pf_q\,G^{(2,1)}(C_q,T)\,{}_qf_{p_i}\,dp\,dq + \\
&+\int_0^\infty \sum_b {}_{p_i}f_p\,G^{(2,1)}(C_p,T)\,{}_pl_b\,G^{(2,1)}(C_b,T)\,{}_bl_{p_i}\,dp \\
&+\sum_b\int_0^\infty {}_{p_i}l_b\,G^{(2,1)}(C_b,T)\,{}_bl_q\,G^{(2,1)}(C_q,T)\,{}_qf_{p_i}\,dq \\
&+\sum_b\sum_{b'} {}_{p_i}l_b\,G^{(2,1)}(C_b,T)\,{}_bj_{b'}\,G^{(2,1)}(C_{b'},T)\,{}_{b'}l_{p_i}
\end{aligned}
\right\}
\tag{16}
$$

with ${}_bj_{b'} = \langle\phi_b|\exp(-2\,\chi z)|\phi_{b'}\rangle$.

The functions $G^{(2,1)}$ are those which appear in the one phonon exchange of the second order term. Thus, two such G functions account for two successive single phonon exchanges.
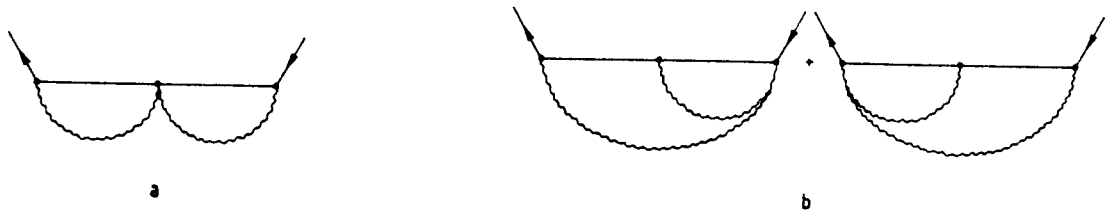

Fig. 2. — Third order diagrams with two virtual phonon process.

— diagram 2b :

$$_iF_i^{(3,2)} = 4(A^2 D)^3 \left[\int_0^x \int_0^x {}_pf_p\, {}_pf_q (G^{(3,2)}(C_p, C_q, T) + G^{(3,2)}(C_q, C_p, T))\, {}_qf_{p_i}\, dp\, dq + \right.$$

$$\left. + \text{ terms arising from other possible intermediate states as in Eq. (16)} \right] \qquad (17)$$

where :

$$G^{(3,2)}(C_2, C_1, T) = 4\frac{m}{M} \int_{-\Omega_m}^{+\Omega_m} \frac{\rho(\Omega)}{\Omega} \langle\!\langle n(\Omega) \rangle\!\rangle \frac{d\Omega}{C_2 + \Omega + i\varepsilon} G^{(2,1)}(C_1 + \Omega, T). \qquad (18)$$

The sum of $G^{(3,2)}$ functions correspond to the sum of the two symmetric diagrams.

The $G^{(3,2)}$ factor clearly reproduces the form of diagrams 2b. With the $G^{(2,1)}$ function in (18) we have two phonon exchange (see expression (15)) located at one of the diagram extremities. The phonon Ω' contained in $G^{(2,1)}$ is then exchanged on the intermediate vertex and the phonon Ω is itself exchanged on the other diagram extremity.

Note that expansion to higher order of the W functions in $W(t_2, t_1)$ will yield diagrams with at least three phonon exchange.

6. Fourth order term.

The fourth order term in expansion (5) is, after the thermal averaging :

$$\langle\!\langle {}_iT_i^{(4)} \rangle\!\rangle = \left(\frac{-i}{\hbar}\right)^3 D^4 \iiint_0^\infty \exp(-2\chi z)\exp[(ic - \varepsilon)t_3/\hbar]\exp(-2\chi z)\exp[(ic - \varepsilon)t_2/\hbar] \times$$

$$\times \exp(-2\chi z)\exp[(ic - \varepsilon)t_1/\hbar]\exp(-2\chi z)\, W(t_3, t_2, t_1)\, dt_3\, dt_2\, dt_1$$

where $W(t_3, t_2, t_1)$, after some algebric transformation, is given by

$$W(t_3, t_2, t_1) = (W(t_3, 0)\, W(t_3 + t_2, 0)\, W(t_1 + t_2 + t_3, 0) - 1) \times$$

$$\times [(W(t_2, 0)\, W(t_1, 0) - 1)(W(t_1 + t_2, 0) - 1) + (W(t_2, 0) - 1)\, W(t_1, 0) - 1)]$$

$$+ (W(t_1 + t_2 + t_3, 0) - 1)(W(t_3 + t_2, 0) - 1)(W(t_3, 0) - 1)$$

$$+ W(t_1 + t_2 + t_3, 0)\, W(t_3 + t_2, 0)(W(t_1, 0) - 1)(W(t_3, 0) - 1)$$

$$+ W(t_3, 0)\, W(t_1 + t_2 + t_3, 0)(W(t_1 + t_2, 0) - 1)(W(t_3 + t_2, 0) - 1)$$

$$+ W(t_3, 0)\, W(t_3 + t_2, 0)(W(t_2, 0) - 1)(W(t_1 + t_2 + t_3, 0) - 1).$$

By expanding the W functions one can see that the first and second terms in $W(t_3, t_2, t_1)$ give diagrams of at least three phonon exchange. The two phonon diagrams come only from the three last term. The corresponding exponentials which enter into the different t integrations are :

$$\exp(i\Omega_2 \tau_3)\exp(i\Omega_1 \tau_1) \qquad \qquad (a)$$

$$\exp(i\Omega_1(\tau_3 + \tau_2))\exp(i\Omega_2(\tau_2 + \tau_1)) \qquad \qquad (b)$$

$$\exp(i\Omega_1 \tau_2)\exp(i\Omega_2(\tau_1 + \tau_2 + \tau_3)). \qquad \qquad (c)$$

The corresponding diagrams are depicted in figure 3a, b and c. For the sake of convenience we shall label them as « spectacle », « exchange » and « direct » diagrams respectively. As there are three propagators in this fourth order term, one should introduce three projectors. Thus each $\langle\!\langle T \rangle\!\rangle$ matrix element contains eight terms, each composed of four matrix elements f, l or j multiplied by an appropriate $G^{(4,2)}$ function. This function must be calculated in each case and if possible with the help of the preceeding ones.

— « Spectacle » diagram :

It is composed of two single phonon diagrams separated by a free or elastic propagator. Thus it is straightforward to calculate the $\langle\!\langle T \rangle\!\rangle$ matrix element which is equal to :

$$_iF_i^{(4,2)} = \frac{1}{4}\left[\int_0^\infty dp\, F^{(2,1)}(p_i p)\frac{1}{C_p + i\varepsilon}F^{(2,1)}(pp_i) + \sum_b F^{(2,1)}(p_i b)\frac{1}{C_b}F^{(2,1)}(b, p_i) \right] \qquad (19)$$
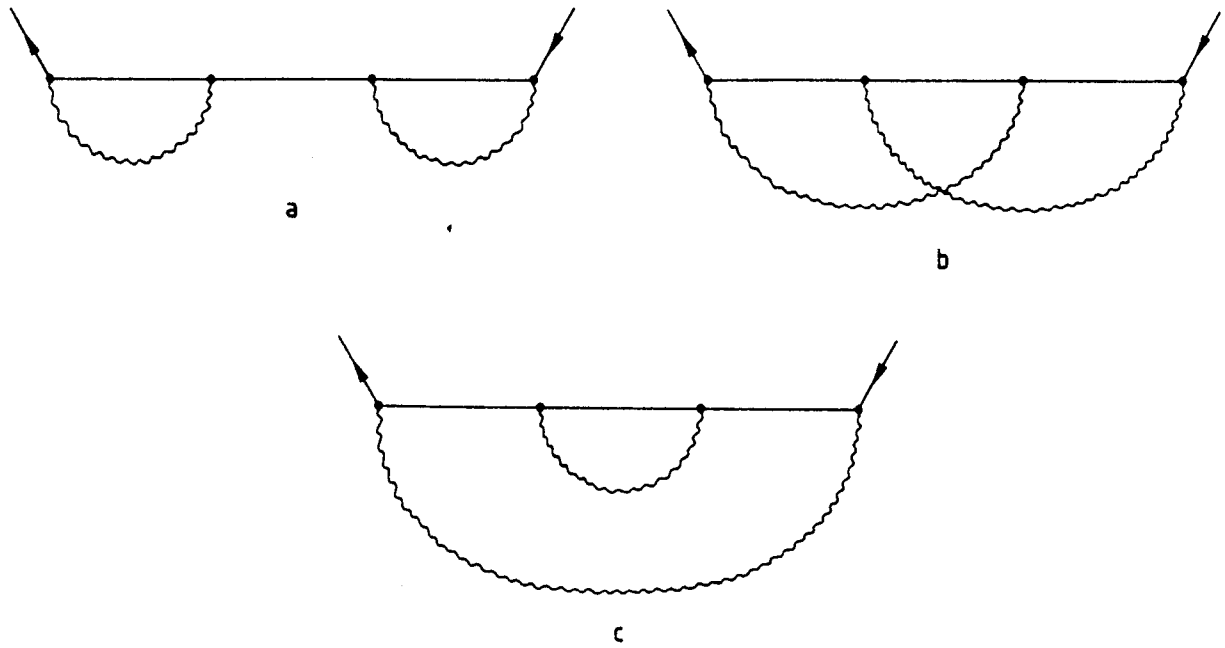
Fig. 3. — Fourth order diagrams with two virtual phonon process. a) « spectacle », b) « exchange ». c) « direct ».

where $F^{(2,1)}(p_i p)$ or $F^{(2,1)}(p_i b)$ and the reverses $F^{(2,1)}(pp_i)$ or $F^{(2,1)}(bp_i)$ are respectively the matrix element of single phonon exchange between initial state p or b and final state p_i and the matrix element of the reverse process.

These different quantities are given by expression (11) in which p_i has to be replaced by p or b at the appropriate place. As $F^{(2,1)}(p_i p)$ or $F^{(2,1)}(p_i b)$ contains two parts $_iF_i^{(4,2)}$ consists of eight different terms.

It is interesting to note that the integration over p leads to

$$- i\pi(_iF_i^{(2,1)}(p_i p_i))^2 + \text{principal value}$$

where the coefficient of $- i\pi$ is the square of the one phonon matrix element.

— « Exchange diagram » :

For simplicity we write only the component in the $\ll T \gg$ matrix element corresponding to transition via continum states. After performing the three integration one gets :

$$_iF_i^{(4,2)} = 4(A^2 D)^4 \iiint_0^\infty {}_pf_p \,{}_pf_q \,{}_qf_r \,{}_rf_{p_1}\, G^{(4,2)}(C_p, C_p, C_r, T)\, dp\, dq\, dr \qquad (20)$$

with

$$G^{(4,2)} = \left(\frac{4\,m}{M}\right)^2 \int_{-\Omega_m}^{+\Omega_m} \int_{-\Omega_m}^{+\Omega_m} \frac{\rho(\Omega_1)}{\Omega_1} \ll n(\Omega_1) \gg \frac{\rho(\Omega_2)}{\Omega_2} \ll n(\Omega_2) \gg \frac{1}{C_p + \Omega_1 + i\varepsilon} \times$$

$$\times \frac{1}{C_q + \Omega_2 + \Omega_1 + i\varepsilon} \frac{1}{C_r + \Omega_2 + i\varepsilon} d\Omega_1\, d\Omega_2 . \qquad (21)$$

The three Green factors could be transformed easily into :

$$\left(\frac{1}{C_p + \Omega_1 + i\varepsilon} + \frac{1}{C_r + \Omega_2 + i\varepsilon}\right)\left(\frac{1}{C_q + \Omega_1 + \Omega_2 + i\varepsilon} - \frac{1}{C_r + C_p + \Omega_1 + \Omega_2 + 2\,i\varepsilon}\right)\frac{1}{C_r + C_p - C_q + i\varepsilon}$$

and the Ω integration leads to :

$$G^{(4,2)} = \frac{1}{C_r + C_p - C_q + i\varepsilon} [G^{(3,2)}(C_p, C_q, T) + G^{(3,2)}(C_r, C_q, T) -$$

$$- G^{(3,2)}(C_p, C_r + C_p, T) - G^{(3,2)}(C_r, C_r + C_p, T)] . \qquad (21)$$

The $G^{(3,2)}$ function is already defined in equation (18). Now in the integration over q in equation (20) the factor $- i\pi(C_r + C_p - C_q)$ gives obviously zero and only the principal value yields a contribution.

In order to get the total dimensionless $_iF_i^{(4,2)}$ matrix element it is necessary to add to (20) :

— three terms with one bound state in place of p, q and r, respectively,
— three terms with two bounds states in place of pq, qr and pr, respectively,
— and one term with three bound states.
— « Direct diagram » :

The $\ll {}_iT_i \gg$ matrix element for this diagram has the same form as the « exchange » one. The $G^{(4,2)}$ function is different and given by :

$$G^{(4,2)} = \left(\frac{4\,m}{M}\right)^2 \iint_{-\Omega_m}^{+\Omega_m} \frac{\rho(\Omega_1)}{\Omega_1} \ll n(\Omega_1) \gg \frac{\rho(\Omega_2)}{\Omega_2} \ll n(\Omega_2) \gg \times$$

$$\times \frac{1}{C_p + \Omega_2 + i\varepsilon} \frac{1}{C_q + \Omega_1 + \Omega_2 + i\varepsilon} \frac{1}{C_r + \Omega_2 + i\varepsilon} d\Omega_1\, d\Omega_2 . \qquad (22)$$

The integration over Ω_1 gives :

$$G^{(4,2)} = \left(\frac{4\,m}{M}\right)^2 \int_{-\Omega_m}^{+\Omega_m} \frac{\rho(\Omega_2)}{\Omega_2} \ll n(\Omega_2) \gg \frac{1}{C_p + \Omega_2 + i\varepsilon} \frac{1}{C_r + \Omega_2 + i\varepsilon} G^{(2,1)}(C_q + \Omega_2, T)\, d\Omega_2$$

and the remaining integration is performed using the usual method of integration employed in the case of a single factor $\dfrac{1}{C + \Omega + i\varepsilon}$. On gets

$$G^{(4,2)} = [G^{(3,2)}(C_p, C_q, T) - G^{(3,2)}(C_r, C_q, T)] \frac{1}{C_r - C_p} .$$

If $C_r = C_p$, $G^{(4,2)} = \dfrac{\partial G^{(3,2)}(C_p, C_q, T)}{\partial C_p} .$

7. Extension to higher order or higher phonons processes.

Let us consider a diagram of order α with an exchange of β phonons. It contains α vertices, $(\alpha - 1)$ propagators and β phonon lines, each of them connecting two vertices.

In the associated dimensionless matrix element, associated with each propagator there corresponds univocally an integration over a given τ variable, and to each phonon line a factor $\exp i\Omega(\tau_u + \tau_{u+1} + \cdots + \tau_{u+x})$ where x is equal to the number of propagators comprised between the two connected vertices by this phonon line.

In order to perform the $(\alpha - 1)$ integrations over τ variables, the different $\exp i\Omega_\gamma \tau$ for each τ are collected. This yields for a given τ an integrand equal to

$$\exp((ic - \varepsilon)\tau)\quad \exp i\tau\left(\sum_{\gamma=1}^{s} \Omega_\gamma\right)$$

where s is equal to the number of phonon lines which,

on the diagram, are drawn in front of the propagator corresponding to the variable τ. This yields a Green operator equal to

$$\frac{1}{C + \left(\sum\limits_{\gamma=1}^{s} \Omega_\gamma\right) + i\varepsilon} .$$

To get the complete expression of the matrix element one should introduce $(\alpha - 1)$ projectors. This produces the appearence of $2^{(\alpha-1)}$ terms depicting the different possible ways of transition *via* continuum or bound states. Each of them contains α matrix elements f, l or j with the corresponding integration over continuum states for f or summation over bound states for l and j. This product of matrix element is multiplied by an appropriate $G^{(\alpha,\beta)}$ function which can be written with the help of the above considerations. For instance, for transition by only continum states one gets :

$$F^{(\alpha,\beta)} = 4(A^2 D)^\alpha \underbrace{\int_0^\infty \cdots \int_0^\infty}_{\alpha - 1} p_r f_{p_1}\left(\prod_{n=1}^{\alpha-2} p_r f_{p_{n+1}} dp_n\right) p_\alpha f_{p_1} dp_{\alpha-1} G^{(\alpha,\beta)}(C_1, \ldots, C_{\alpha-1}, T) \qquad (23)$$

with

$$G^{(\alpha,\beta)} = \left(\frac{4\,m}{M}\right)^{\beta} \underbrace{\int_{-\Omega_m}^{+\Omega_m} \cdots \int_{-\Omega_m}^{+\Omega_m}}_{\beta} \left(\prod_{\gamma=1}^{\beta} \frac{\rho(\Omega_\gamma)}{\Omega_\gamma} \ll n(\Omega_\gamma) \gg d\Omega_\gamma\right)$$

$$\left(\prod_{p=1}^{\alpha-1} \frac{1}{C_p + \left(\sum_{\gamma=1}^{s} \Omega_\gamma\right) + i\varepsilon}\right). \tag{24}$$

In this way for a given diagram the associated dimensionless matrix element can be directly written.

8. Conditions for numerical calculation.

Prior to numerical calculation we should ascribe definite values to the potentiel parameters and to the spectral density $\rho(\Omega)$. This last quantity depends only upon the crystal properties.

— Crystal : the type of potential used in writing the different matrix elements is relevant to a flat surface. Such a surface is well represented by the (100) face of FCC crystal like copper. In effect, in helium scattering experiments the diffraction peak intensities are less than 10^{-4} of the specular one (15). Thus we consider this face for the determination of the thermal displacement u of the repulsive part of the potential.

It is well known that in the repulsive region the potential is proportional to the surface electronic density in the first approximation (5). In this way the potential thermal displacement is directly linked to the thermal fluctuation of the electronic density, yielded on a given point by the thermal motion of many surface atoms close to the point considered. In the absence of theoretical calculation of this effect we propose to model it by taking a displacement u equal to the mean displacement of the four atoms belonging to the (100) cell. Due to the one dimensionality of the potential model we consider only the normal displacement to the (100) face. This gives :

$$u = \frac{1}{4}(u_1^{ZZ} + u_2^{ZZ} + u_3^{ZZ} + u_4^{ZZ})$$

and we get for the thermal average

$$\langle u(t)\,u(0) \rangle = \frac{1}{4} \langle u_1^{ZZ}(t)\,u_1^{ZZ}(0) \rangle +$$

$$+ \frac{1}{2} \langle u_1^{ZZ}(t)\,u_2^{ZZ}(0) \rangle + \frac{1}{4} \langle u_1^{ZZ}(t)\,u_3^{ZZ}(0) \rangle$$

where the subscripts 1, 2 and 1, 3 label, respectively, the correlated displacement between nearest and next nearest neighbour atoms.

Therefore the spectral density is given by :

$$\rho(\Omega) = \frac{1}{4}\rho_{11}^{ZZ}(\Omega) + \frac{1}{2}\rho_{12}^{ZZ}(\Omega) + \frac{1}{4}\rho_{13}^{ZZ}(\Omega).$$

The different quantities above have been calculated previously [6]. The crystal used for this purpose does not exhibit any surface plane relaxation and takes account only the central force between nearest neighbours.

With this simple model of force the different quantities relative to the crystal are calculated as a function of dimensionless frequencies $\Omega_c = \omega\left(\frac{K}{M}\right)^{1/2}$, where K and M are respectively the force constant and the mass of a crystal atom. In particular the spectral density $\rho(\Omega_c)$ is invariant whatever the K and M values may be.

This allows one to introduce crystal anharmonicity through the quasi-harmonic approximation. For that one considers the variation of the equilibrium distance between atoms with the temperature, and given a central potential interaction, the force constant K is evaluated at this equilibrium distance for each temperature. At a given value of this quantity the crystal properties depending upon phonon frequencies are calculated in the harmonic approximation. The anharmonicity of the atom potential yields a decrease of K values as the temperature increases and this produces a contraction of the real frequency scale characterized by the variation of the maximum frequency.

The effective pair potential has been calculated by one of us [7] for copper and the corresponding maximum frequency variation is depicted in figure 4. For comparison the available experimental data obtained by neutron scattering experiments are also plotted in the same figure. One sees that the available experimental values are very well reproduced.

In this way for our calculation the spectral density $\rho(\omega)$ is given by

$$\rho\left(\omega = \Omega_c\left(\frac{K}{M}\right)^{1/2}\right) = \rho(\Omega_c).$$

Note that this procedure supposes that anharmonicity on the surface is the same as in the bulk.

— Potential : the attractive part of the potential $f(z)$, left undefined in expression (6), enters only in the thermal average potential which has been chosen equal to the distorted potential. In particular, it does
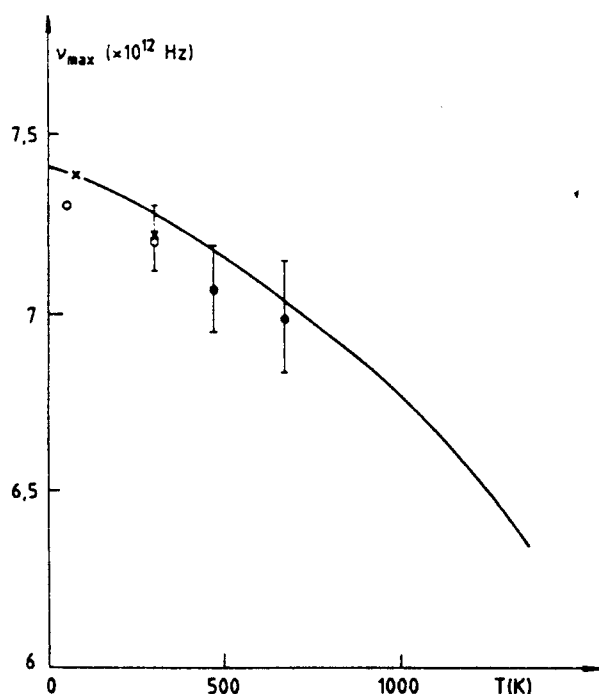
Fig. 4. — Variation of the maximum phonon frequency of Copper as a function of temperature. Experimental data : ⊙ reference [8], × reference [9], ⟡ error bar from reference [10].

not affect the $v(u)$ expression (Eq. (7)) and consequently does not change the analytical form of the different $_iF_i^{(n,m)}$ quantities. Its influence is localized in the matrix element $_pf_q, _pl_b, _bj_b$ through the eigenfunctions of the distorted potential.

One can then infer that the shape of $f(z)$ is amongst the different parameters, the one which has the least influence, except when the normal kinetic energy of the incident particle is low. In this case the transition through bound states gives an important contribution.

For convenience we take $f(z) = 2 e^{-\chi z}$ and the distorted potential is of Morse shape. The total potential (6) could be written as

$$V = D \exp(- 2 \chi u) \exp(2 \chi^2 \ll u^2 \gg) \quad (X^2 - 2 X)$$

with

$$X = \exp(- \chi z) \exp(2 \chi u) \exp(- 2 \chi^2 \ll u^2 \gg).$$

The equipotential is located at

$$z = 2 u - 2 \chi \langle u^2 \rangle - \frac{1}{\chi} \mathrm{Log}\left[1 \pm \left(1 + \frac{V}{D} \times \right.\right.$$

$$\left.\left. \times \exp(2 \chi u) \exp(- 2 \chi \ll u^2 \gg)\right)^{1/2}\right]$$

where the $\pm$ signs stand for $V < 0$. On the contrary the minus sign should be disregarded. Therefore the

potential thermal displacement is equal to

$2 u$ at the bottom of the well

$2 u$ for $V = 0$

u for $\dfrac{V}{D}$ very large .

As the particle incident energy is at most ten times the well depth in the following calculations, it happens that the potential thermal displacement is close to $2 u$. In order to recover the correct displacement one should divide u by 2, that is to say multiply the spectral density by $\alpha = 1/4$. Note that by varying this quantity one can compensate the deficiency of the potential model like, the lack of parallel momentum exchange. In this way its value could be slightly different of $1/4$.

Now the remaining parameter values D and χ are dependent upon the nature of the incident particle. In each of the following cases these values are taken equal to those which give a good fit of the experimental data in an elastic diffraction experiment. They are given in table I.

9. Results.

— Helium-copper system : for an incident energy of 21 meV (wavevector $k_i = 6.4 \text{Å}^{-1}$) figures 5, 6 and 7 give the calculated intensities versus crystal temperature up to 1 350 K, respectively for an incident angle θ_i of 73.5, 55.5 and 31.8 degrees.

The curves are labelled by the symbol AH or H respectively for quasi-harmonic or harmonic calculation. In this last case the maximum crystal frequency is taken equal to 7.3 × 10^{12} Hz. A diagram of order n with m virtual phonons exchanged is denoted (n, m). In this way the curves denoted AH. (2, 1) is the result of one phonon anharmonic calculation, and those labelled AH. (2, 1) + (3, 2) + (4, 2) give the calculated intensity including the whole one and two phonon processes. In this last case two curves could be seen for large incident angles, labelled c or c + b. They give respectively the calculated results including only continum states or continum + bound states. Of course, only one curve is drawn when the effects of bound states are negligeable.

Table I. — Potential parameter values used in the calculation for the different incident particles.

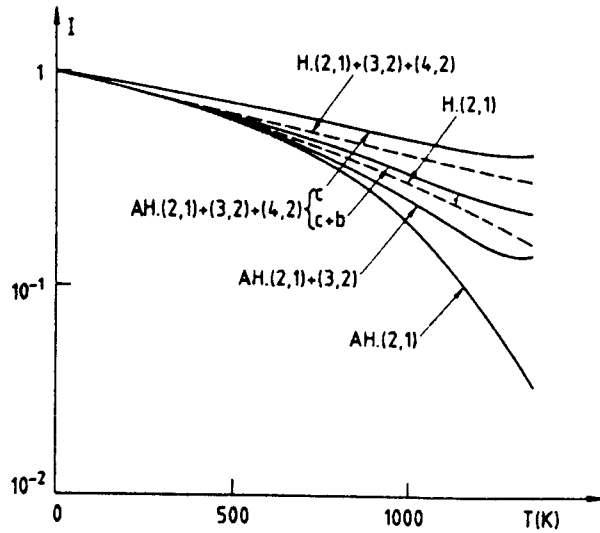| Incident particle	D meV	χ Å^{-1}	Fit on	Reference
He	6.35	1.05	(110), (113), (115), (117)	[11]
H_2	21.6	0.97	(110), (115)	[12]
Ne	12.2	1.9	(110)	[13]

Fig. 5. — Calculated intensity as a function of the crystal temperature. Full line AH — quasi-harmonic calculation. Dashed line H — harmonic calculation. (2, 1) one photon — (2, 1) + (3, 2) one phonon + two phonon of third order — (2, 1) + (3, 2) + (4, 2) all one and two phonon contribution; curve labelled c continum states. c + b continum + bound states He-Cu system, $E_i = 21$ meV, $\theta_i = 73.5$ degrees.
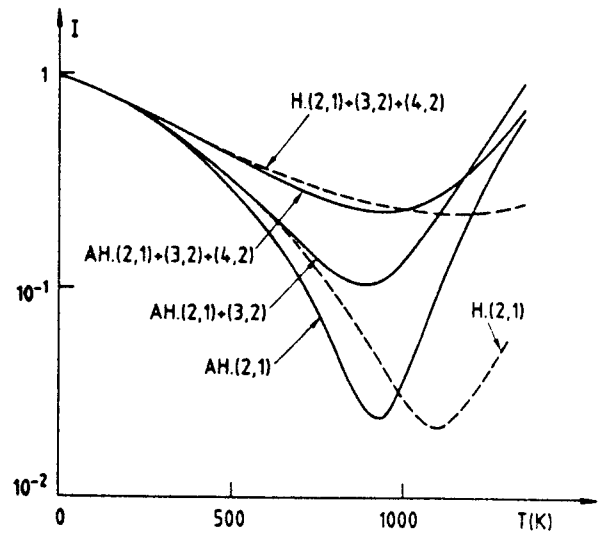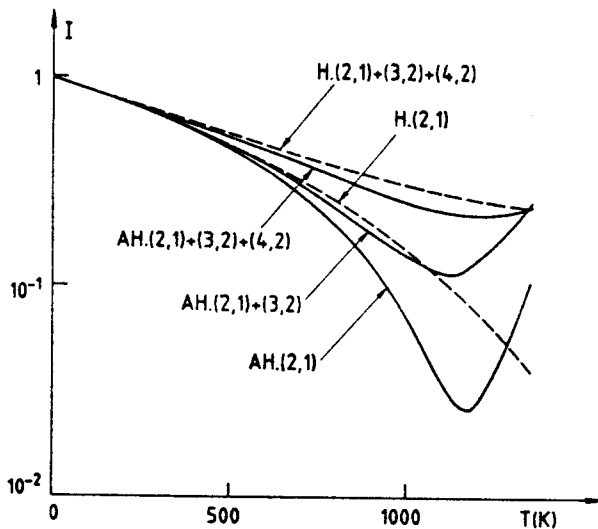

Fig. 6. — Same as 5 but $\theta_i = 55.5$ degrees.

Fig. 7. — Same as 5 but $\theta_i = 31.8$ degrees.
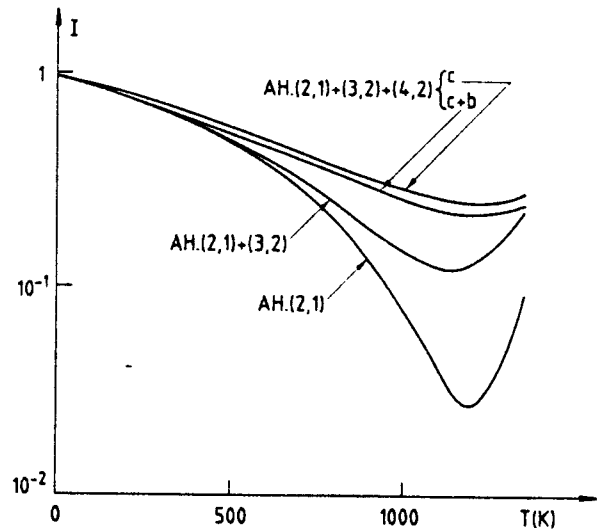
Fig. 8. — Same as 5 but $E_i = 63$ meV, $\theta_i = 71.6$ degrees.
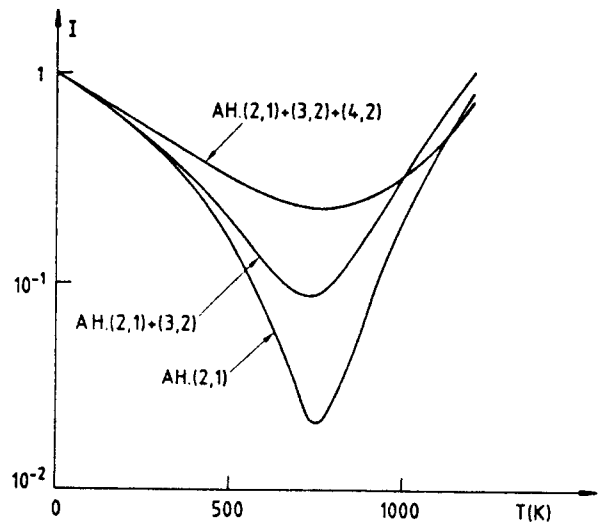

Fig. 9. — Same as 5 but $E_i = 63$ meV, $\theta_i = 51.5$ degrees.

For the same conditions figures 8, 9 and 10 give the results for an incident energy of 63 meV ($k_i = 11$ Å^{-1}), respectively, for incident angles of 71.6, 51.5 and 19 degrees.

— Molecular hydrogen-copper system : with the same notations, figures 11 and 12 give the calculated intensity for molecular hydrogen with an incident energy of 77 meV ($k_i = 8.6$ Å^{-1}), with incident angles of 75.5 and 31 degrees respectively.

The points represent the experimental data [14]. They have been translated along the vertical axis by a factor equal to the lack of unitarity. Note that the sum
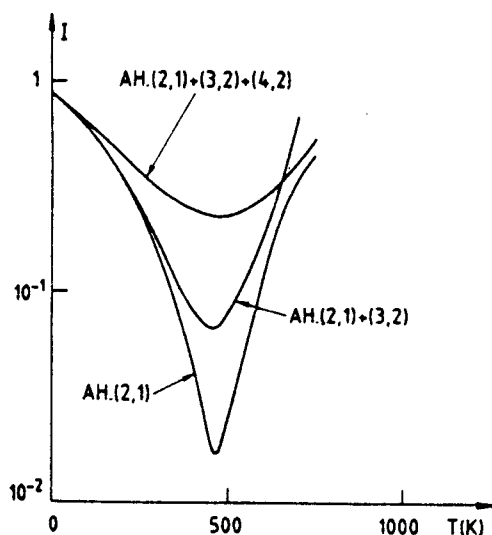
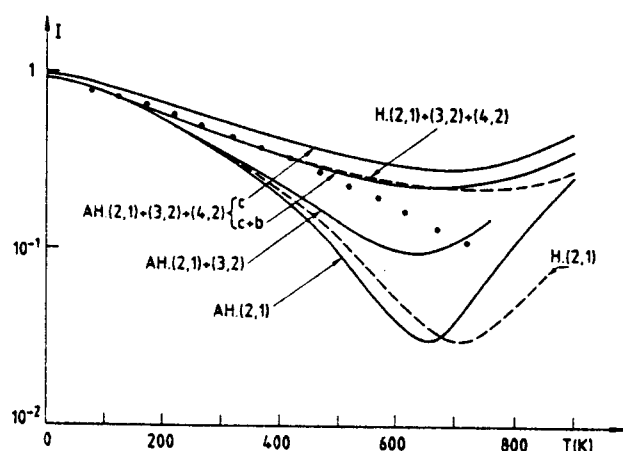Fig. 10. — Same as 5 but $E_i = 63$ meV, $\theta_i = 19$ degrees.

of diffracted peak intensities in this experiment is at most equal to 10^{-2} that is to say 30 times smaller than the measured specular intensity.

— Neon-copper system : the calculation is done with the quasi-harmonic approximation for an incident energy of 63 meV ($k_i = 24.8$ Å^{-1}). Figures 13a, b and c give the results for incident angles of 75, 60 and 45 degrees respectively. As in the case of hydrogen the experimental data [15] has been translated in order to compensate the lack of experimental unitarity.

10. Discussion.

10.1. — The variation of the factor $\dfrac{\rho(\Omega)}{\Omega} \ll n(\Omega) \gg$ as a function of Ω in the interval $-\Omega_m$ to $+\Omega_m$ is represented in figure 14. Note that the ordinate scale is logarithmic and that for $\pm \Omega_m$ this factor is equal to zero. This is not a universal curve as the spectral density varies from face to face for a given body.

Fig. 11. — Same as 5 but H_2-Cu system, $E_i = 77$ meV, $\theta_i = 75.5$ degrees, the points represent the experimental data.
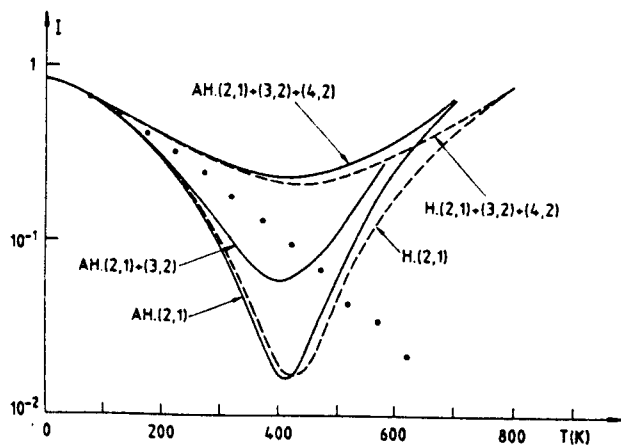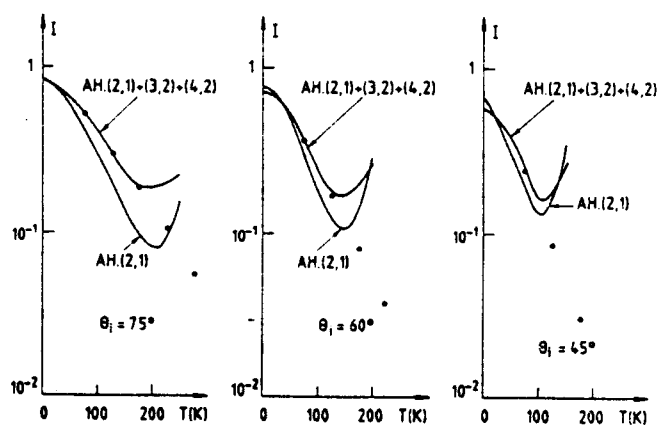
Fig. 13. — Same as 11 but Ne-Cu system, $E_i = 63$ meV, $\theta_i = 75$, 60, 45 degrees.
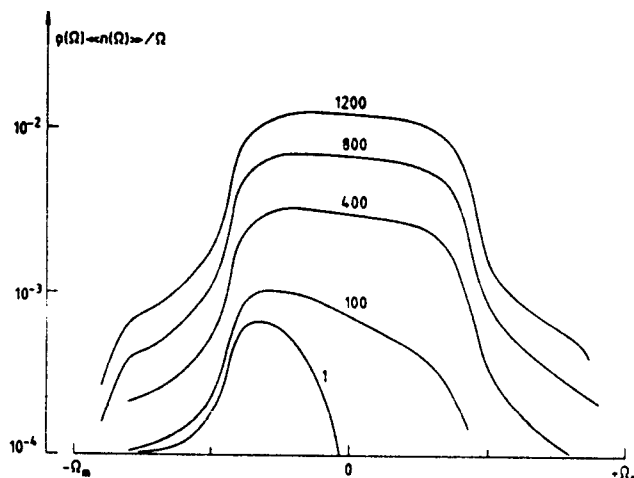
Fig. 12. — Same as 11 but $\theta_i = 31$ degrees.

Fig. 14. — Variation of the frequency factor in the interval $-\Omega_m$, $+\Omega_m$. Each curve is labelled by the crystal temperature.

At low crystal temperature T the phonon creation process is preponderant. At $T = 400$ K and above the curves are almost symmetric with respect to the Ω values : creation and annihilation processes are practically equally probable. More interesting is to observe that above 400 K, 40 to 50 % of the low frequencies will contribute significantly to the scattering process.

This interval could be reduced by the integration over the p variable which introduces the matrix element linked to each vertex. Taking account only of this integration we consider solely the transitions *via* continuum states which are the most efficient processes. In order to illustrate this point let us consider the $(2, 1)$ diagram. The imaginary part of $G^{(2,1)}$ (see formula (12)) is equal to $-i\pi\dfrac{\rho(\Omega)}{\Omega} \langle\!\langle n(\Omega) \rangle\!\rangle$ with $\Omega = p^2 - p_i^2$. As p varies around p_i this factor remains practically constant as long as the corresponding Ω value falls into the Ω interval defined above. In the p integration this factor is multiplied by the square of the matrix element $_p f_p$ which is maximum for $p \simeq p_i$ and decreases as the quantity $|p - p_i|$ increases. This would yield a reduction of the low frequency domain giving the main contribution to the scattering process.

In order to verify this fact the calculation has been done for the scattering of H_2 keeping only $\pm X \%$ of the low phonon frequencies. With $X = 40$ the intensity *versus* temperature curves could be superimposed over that calculated with $X = 100$. Taking $X = 30$ the calculated intensities are approximatly 10 % higher. Therefore the bound state resonance could be an efficient process if the normal kinetic energy of the incident particle $E_\perp$ is less than 30 % or 60 % of the maximum phonon energy respectively for the one and one plus two phonon processes. For copper the two corresponding values are, respectively, 9 and 18 meV. The numerical results presented above confirm this view.

We should outline that this effect is a consequence of the structure of the correlated displacement and of the shape of the matrix element attached to each vertex. Thus one can expect that the same limitation in the phonon efficiency can happen with a three dimensional potential allowing the exchange of parallel momentum. As the phonons of low frequency have also low parallel momentum, the exchange of this quantity will be limited to a more or less extended domain of the Brillouin zone around its center. This expectation tends to justify the use of a one dimensional potential such as we have chosen, and to understand its success in the representation of experimental data for scattering by a flat surface.

10.2. — The different expressions giving the $\langle\!\langle {}_i T_i^{(\alpha,\beta)} \rangle\!\rangle$ matrix element written above for β equal 1 or 2, and the rule allowing one to write the matrix element for diagrams of higher order, show that for a virtual exchange of β phonons there are β integrations over Ω variables, each of them containing the Bose-Einstein factor $\langle\!\langle n(\Omega) \rangle\!\rangle$. At sufficiently high temperature T, $\langle\!\langle n(\Omega) \rangle\!\rangle$ is proportional to $kT/\hbar\omega$ and therefore the $\langle\!\langle {}_i T_i^{(\alpha,\beta)} \rangle\!\rangle$ matrix element is proportional to T^β whatever the diagram order α may be. The ratio $R_T = \langle\!\langle {}_i T_i^{(\alpha,\beta)} \rangle\!\rangle / T^\beta$ should be constant at high temperature. One verifies this statement in harmonic calculation where one finds that R_T tends asymptotically to a constant as T increases. This is not the case in the quasi-harmonic calculation due to the variation of Ω_m with T. But the comparison of the ratio values calculated at high temperature for different diagrams with the same β value, allows one to appreciate the efficiency of each of them. Tables II to V give the R_T values for the different cases studied here.

Looking for the moment to the absolute value of the real and imaginary parts of this ratio one can put the different two phonon diagrams in the following decreasing order of importance : « spectacle », « exchange », « direct », $\smile\smile$, $\bigcirc\!\!\!\smile = \smile\!\!\!\bigcirc$, $\boxdot$.

This order is independent of the nature of the incident particle and of the experimental condition (E_i, θ_i). One notices that this classification coincides with that obtained by taking the decreasing order of the diagram order.

We have pointed out in paragraph 7 that the Green operator corresponding to a propagator is equal to $\left(C_{p_b} + \displaystyle\sum_{\gamma=1}^{s} \Omega_\gamma + i\varepsilon \right)^{-1}$, where s is the number of phonon lines associated with the propagator in a diagram. One can think that as s increases the contribution of the Green function in the different Ω integrations decreases. Thus the efficiency of a diagram could be inversely proportional to the sum of s values relative to each propagator say $S = \displaystyle\sum_{1}^{\alpha-1} s$. With this assumption we tentatively compare the efficiency of diagrams belonging to the same order. This last condition is required by the subsequent integration or summation over the product of matrix elements f, l or j by $G^{(n,m)}$ functions, which for comparison should be identical.

For the $(3, 2)$ diagrams we have :

$$\smile\smile \quad S = 2, \qquad \bigcirc\!\!\!\smile = \smile\!\!\!\bigcirc \quad S = 3 .$$

Effectively the ratio R_T is greater for the former than the latter. Let us now make a quantitative comparison by looking at the ratio $R_{T\,\smile\smile}/R_{T\,\smile}$ given in the tables. One observes that these values (real or imaginary part) are located between

$$
\begin{aligned}
&1.23 - 1.9 && \text{for} && \text{He-Cu system} \\
&1.37 - 1.72 && \text{for} && \text{Ne-Cu system} \\
&1.06 - 1.33 && \text{for} && H_2\text{-Cu system}
\end{aligned}
$$

and that it decreases as the incident angle decreases for each system. By definition these values are independent of the mass of the incident particle and their

Table II. — *Real and imaginary part of R_T which is equal to the ratio of the diagram T matrix element to the temperature T (2, 1) or to the square of the temperature T^2 for the others. — n stands for 10^{-n}. He-Cu systems — E_i = 21 meV — T = 1 000 K; in case of two values :*

$$\begin{cases} \text{the first is with continum states} \\ \text{the second is with continum + bound states.} \end{cases}$$

He-Cu	Diagram		$E_i = 21$ meV $\theta_i = 73.5$, $E_\perp = 1.69$		$\theta_i = 55.5$, $E_\perp = 6.73$		$k_i = 6.4\,\text{Å}^{-1}$ $\theta_i = 31.8$, $E_\perp = 15.16$	
(2, 1)	▽		− 0.231-3	− 1.239-3	− 0.577-3	− 3.377-3	− 1.081-3	− 7.182-3
(2, 2)	▤		− 0.205-8	− 0.117-7	− 0.524-8	− 0.319-7	− 0.103-7	− 0.687-7
(3, 2)	◡◡▽		− 0.647-7	0.388-7	− 0.215-6	0.111-6	− 0.558-6	0.241-6
(3, 2)	▽ = ▽		− 0.406-7	0.206-7	− 0.139-6	0.655-7	− 0.383-6	0.158-6
	◡◡ / ▽		1.59	1.88	1.546	1.698	1.456	1.525
(4, 2)	▽◡▽	c	0.316-6	0.134-6	0.755-6	0.395-6	0.147-5	0.163-5
		c + b	0.279-6	− 0.160-6				
(4, 2)	◡◡◡	c	0.694-7	0.184-7	0.289-6	0.254-6	0.820-6	0.885-6
		c + b	0.790-7	0.584-7				
(4, 2)	◡◡	c	0.399-7	0.267-7	0.200-6	0.188-6	0.632-6	0.701-6
		c + b	0.465-7	0.424-7				
	▽▽ / ◡◡◡		3.53		2.612	1.555	1.792	1.84
	▽▽ / ◡◡		6		3.775	2.10	2.32	2.32

variation from one system to another should be ascribed to the potential parameters, the well depth D and exponential damping coefficient χ. For the He and H_2 scattering the χ values are not very much different. Thus it seems that well depth is the most important parameter yielding a decrease of the ratio when D increases. Following the preceding rule the ratio value should be equal to 1.5 a value which is outside of the variation interval for hydrogen-copper system.

Let us now consider the (4, 2) diagrams. We have : « spectacle » $S = 2$, « exchange » and « direct » $S = 4$. Here the ratio R_T spectacle/R_T exchange and R_T spectacle/R_T direct should be equal to 2. From the tables one gets a variation between

Ex	1.28 − 3.53	He-Cu
Di	1.47 − 6	
Ex	1.55 − 2.63	Ne-Cu
Di	1.93 − 4.05	
Ex	1.1 − 2.39	H_2-Cu
Di	1.1 − 3.1	

The same comment as in the case of (3, 2) diagrams is valid. However here the « theoretical » value 2 falls into all of the variation intervals which are larger than those of the (3, 2) diagrams. Also there is a singularity at large incident angle for He-Cu (21 meV) and H_2-Cu system : the imaginary part of the R_T value is negative for the « spectacle » diagram. As shown in the table, this is typically an effect of bound state resonances, the R_T value being positive when this effect is suppressed.

To conclude this particular point one can say that the contribution of a diagram to the final intensity increases with the diagram order at a constant number of virtual phonons exchanged. For a given order, the S value gives qualitatively a measure of this contribution which decreases as S increases.

We now consider the sign of the R_T values in connection with the intensity. The total matrix element could be written :

$$F = F^{(2,1)} + F^{(2,2)} + F^{(3,2)} + F^{(4,2)} \bullet$$

Table III. — *Same as 2 but* E_i = 63 meV.

He-Cu		E_i = 63 meV				k_i = 11 Å^{-1}	
Diagram		θ_i = 71.6 $E_\perp$ = 5.18		θ_i = 51.5 $E_\perp$ = 24.41		θ_i = 19 $E_\perp$ = 56.3	
(2, 1)		− 0.544-3	− 3.141-3	− 1.564-3	− 11.675-3	− 3.233-3	− 30.71-3
(2, 2)		− 0.490-8	− 0.297-7	− 0.159-7	− 0.113-6	− 0.361-7	− 0.314-6
(3, 2)		− 0.196-6	0.103-6	− 1.04-6	0.388-6	− 3.59-6	1.02-6
(3, 2)		− 0.127-6	0.060-6	− 0.747-6	0.276-6	− 2.85-6	0.831-6
		1.543	1.716	1.4	1.405	1.26	1.23
(4, 2)		0.707-6	0.318-6	2.515-6	3.367-6	7.773-6	14.338-6
(4, 2)		0.262-6	0.225-6	1.594-6	2.030-6	6.08-6	10.53-6
(4, 2)		0.180-6	0.167-6	1.321-6	1.666-6	5.304-6	9.353-6
		2.7	1.41	1.57	1.66	1.28	1.36
		3.92	1.90	1.9	2	1.47	1.53

Table IV. — *Same as 2 but* H_2-Cu *system*, E_i = 77 meV.

H_2-Cu			E_i = 77 meV		k_i = 8.6 Å^{-1}	
Diagram			θ_i = 75.5 $E_\perp$ = 3.95		θ_i = 31 $E_\perp$ = 46.28	
(2, 1)			− 0.731-3	− 4.402-3	− 2.594-3	− 2.510-2
(2, 2)			− 0.625-8	− 0.357-7	− 2.712-8	− 3.075-7
(3, 2)			− 0.368-6	0.164-6	− 2.688-6	0.735-6
(3, 2)			− 0.277-6	0.128-6	− 2.332-6	0.691-6
			1.328	1.281	1.152	1.063-6
(4, 2)		c	0.198-5	+ 1.481-6	6.056-6	11.487-6
		c + b	0.214-5	− 0.428-8		
(4, 2)		c	0.104-5	− 0.115-6	5.486-6	9.577-6
		c + b	0.826-6	0.826-6		
(4, 2)		c	0.789-6	− 0.210-8	5.328-6	8.975-6
		c + b	0.637-6	0.760-6		
			2.397		1.104	1.2
			3.108		1.136	1.279

Table V. — *Same as 2 but* Ne-Cu *system*, E_i = 63 meV.

Ne-Cu		$\theta_i = .75$ $E_\perp = 4.22$		$\theta_i = 60$ $E_\perp = 15.75$		$\theta_i = 45$ $E_\perp = 31.5$	
Diagram							
(2, 1)	▽	− 0.376-2	− 2.281-2	− 0.913-2	− 6.129-2	− 1.565-2	− 11.94-2
(2, 2)	▽	− 0.112-6	− 0.629-6	− 0.288-6	− 1.719-6	− 0.525-6	− 3.364-6
(3, 2)	▽▽	− 0.655-5	0.286-5	− 0.217-4	0.805-5	− 0.493-4	0.157-4
(3, 2)	▽ = ▽	− 0.403-5	0.167-5	− 0.142-4	0.528-5	− 0.344-4	0.114-4
	▽▽ / ▽	1.625	1.712	1.528	1.524	1.433	1.377
(4, 2)	▽▽	0.269-4	0.241-4	0.706-4	1.106-4	0.145-3	0.272-3
(4, 2)	▽	0.102-4	0.120-4	0.378-4	0.530-4	0.934-4	0.154-3
(4, 2)	▽	0.664-5	0.830-5	0.282-4	0.397-4	0.749-4	0.124-3
	▽▽ / ▽	2.637	2.08	1.86	2.08	1.552	1.766
	▽▽ / ▽	4.05	2.90	2.50	2.785	1.935	2.19

and the reflection coefficient is given by

$$_iR_i = \left(1 + \frac{\pi}{4 p_i} \text{Im}(F)\right)^2 + \frac{\pi^2}{16 p_i^2}(\text{Re}(F))^2$$

where Re and Im stand respectively for the real and imaginary part of F.

Let us consider first the one phonon process alone. The tables II to V show that all the Re (F) and Im (F) are negative and

$$_iR_i^{(1)} = \left[1 - \frac{\pi}{4 p_i} |\text{Im}(R_T^{(2,1)})| \, T\right]^2 +$$
$$+ \frac{\pi^2}{16 p_i^2}[|\text{Re}(R_T^{(2,1)})| \, T]^2 .$$

Such a function of the variable T has the behaviour depicted by the different figures. The minimum occurs at a temperature

$$T = \frac{4 p_i}{\pi} \frac{|\text{Im} \, R_T^{(2,1)}|}{|R_T^{(2,1)}|^2} .$$

This is clear from a mathematical point a view. From the physical view point the existence of this minimum certainly means that well before it occurs the contributions of the 2, 3... phonons processes are not negligible as demonstrated by the respective position of the one and one + two phonon curves.

The (2, 2) diagram like the (2, 1) yields T matrix elements which are always negative. Thus it produces a decrease of the intensity given by the (2, 1). The effect is very small and negligeable except at very high temperature.

The T matrix elements of the (3, 2) diagrams have a negative real part and a positive imaginary one. For the (4, 2) diagrams the real and imaginary parts of their T matrix elements are positive. Thus the total reflection coefficient appears as :

$$_iR_i^{(1,2)} = \left[1 - \frac{\pi}{4 p_i}(|\text{Im}(R_T^{(2,1)})| \, T + (|\text{Im}(R_T^{(2,2)})| - |\text{Im}(R_T^{(3,2)})| - |\text{Im}(R_T^{(4,2)})|) \, T^2)\right]^2 +$$
$$+ \frac{\pi^2}{16 p_i^2}[\text{Re}(R_T^{(2,1)}) \, T + (|\text{Re}(R_T^{(2,2)})| + |\text{Re}(R_T^{(3,2)})| - |\text{Re}(R_T^{(4,2)})|) \, T^2]^2 .$$

The imaginary part coming from the (3, 2) and (4, 2) diagrams yields an increase of the intensity given by the (2, 1) although their real part produces an inverse effect $| \text{Re}(R_T^{(3,2)}) | - | \text{Re}(R_T^{(4,2)}) |$ being negative. The different curves show that the imaginary parts yield the dominant effect and that the (4, 2) diagrams have the major influence in agreement with the order of diagram efficiency.

As in the case of the one-phonon process one observes a minimum in the intensity when the two-phonon processes are added, located at approximately the same temperature. Therefore one can expect that the three-phonon processes will be important at a temperature lower than that of the minimum.

The above analysis based on the sign of the R_T ratio is in principle valid for high temperature, say above 400 K. However the intensities corresponding to the 1 and 1 + 2 phonon processes behave in the same way below 400 K. At very low temperature the inverse behaviour is clearly apparent in the case of the Ne-Cu system. It arises also for the other systems but the difference is so low that it cannot be seen in the figures.

A quick examination of the different figures allows one to determine the crystal temperature T_2 from which the two-phonon processes begin to be influential. Table VI gives these values. T_2 is equal to zero for the Ne-Cu system. For the others, as expected, T_2 decreases as the incident angle decreases or the incident energy increases.

11. Comparison to experimental results.

The intensity of the specular peak in the scattering of helium by a copper (100) surface has been measured again recently [16] in an extended domain of temperature practically up to the melting point. Within experimental uncertainties the results are comparable to the previous one [15]. As these values are in agreement with the calculated one phonon intensities [1, 2] the domain of agreement should be restricted to temperatures below T_2.

For the scattering of molecular hydrogen the measured data [14] fall on the calculated one plus two phonon curves at one incident angle of 75.5 degrees up to a temperature of 500 K (Fig. 11). For the lower incident angle (Fig. 12) the experimental data fall between the one and one plus two phonon theoretical curves.

In the case of neon the one plus two phonon calculation seems to be in agreement with the experimental data [15]. However, the domain of temperature where the comparison could be made is restricted to low temperature values. As discussed above in this temperature range the three or higher phonon processes could modify the calculated intensities. Thus more precise comparison should be postponed until the influence of the higher phonon processes has been calculated.

Table VI. — *Temperature T_2 at which the two phonon processes give a non-negligible contribution to the calculated intensity.*

	E_i	θ_i	T_2
He-Cu	21 meV	73.5	450
		55.5	300
		31.8	250
	63 meV	71.6	400
		51.5	180
		19	100
H$_2$-Cu	77 meV	75.5	150
		31	100
Ne-Cu	63 meV	$\forall \theta_i$	0

Nevertheless, on the whole, the agreement seems to be good in the temperature domain where the present calculation is valid. Unfortunatly, the temperature T_3 from which the three phonon diagrams will influence the intensity is difficult to appreciate. One knows that its value is below the temperature for which a minimum of intensity is observed. Thus the hydrogen case seems to indicate that the introduction of the three phonon diagrams in the calculation should yield a decrease of the calculated intensity.

An important point should now be outlined. The bound state energy levels are determined in an elastic experiment by the observation of elastic resonances and the zero order Fourier component of the potential is then deduced. The potential so determined is not always unique and is usually open to the possible existence of a deeper level, for example a level which is not clearly resolved in the measurement. This has been suggested to be the case for the hydrogen and neon copper systems. For instance the existence of a level at 26 meV for hydrogen is not precluded [17]. This would give a well depth of 32 meV. With such a value the calculated intensities will be lower than those obtained here with $D = 21.6$ meV and the difference will be important due to the major influence of the D value on scattered intensity [2]. However, because we get theoretical intensities comparable to experiment, the thermal attenuation calculations confirm the chosen well depth values.

This analysis suggests that measurements of the thermal attenuation are an extremely useful check on the choice of well depth for a particular system. In fact such a measurement could be used to determine which of several possible values of the well depth is correct.

12. Conclusions.

We are now able to calculate exactly the elastic or inelastic T matrix elements in a scattering process.

The adequacy of the calculated cross section or elastic intensity depends now only upon the chosen potential. A given potential is in fact a more or less good representation of the physical reality.

In this paper all the elastic T matrix elements containing one or two virtual phonon processes have been written down explicitely with a one dimensional soft potential modelling a flat surface. It therefore precludes the exchange of parallel momentum.

The results show that phonons of low frequencies are the most efficient in attenuating the elastic scattering. As they correspond in the crystal to phonons of low parallel momentum we can expect a small exchange of this quantity on a flat surface. For this reason a one dimensional potential can give a good representation of the inelastic scattering attenuation phenomena.

M and m being respectively the mass of a crystal atom and the mass of the incident particle, the T matrix elements are proportional respectively to m/M and $(m/M)^2$ for the one and two phonon events. At high crystal temperature T they are also proportional respectively to T and T^2. Moreover they are strongly dependent upon the well depth value and the exponential damping coefficient of the potential repulsive part. Thus the resulting specular intensity varies strongly from one particle-crystal system to another. In particular, the temperature above which the two phonon effect is appreciable varies from 0 K for the neon-copper system up to 500 K in the case of helium scattered at large incident angle. Its variation with the nature of the incident particle and the different experimental parameters are in conformity with what is expected on an intuitive basis.

Contrary to what is perhaps an intuitive prediction, the inclusion of the two phonon processes generally leads to an increase of the calculated elastic intensity except at very low temperature. This increase, from a physical standpoint, appears to be due to the fact that the dominant effect of the two phonon processes is to reduce the unitarity defect of the total (elastic plus inelastic) single phonon processes. As the inelastic phonon events are well accounted for by second order perturbation theory the restoration of the unitarity modifies the elastic intensity which becomes bigger.

This can be compared to a similar occurrence in ordinary Debye-Waller factor which can be developed as follows :

$$e^{-2W} = 1 - 2W + \frac{(2W)^2}{2!} + \cdots .$$

In the above equation the different terms correspond respectively to 0, 1, 2... virtual phonon processes. It is clear that the two phonon events raise the intensity given by the one phonon alone.

The total calculated intensities for the different particle-crystal pairs are, on the whole, in agreement with the experimental data below the temperature where higher phonon processes are negligible. Depending on the system studied, multiple virtual phonon exchange could yield an appreciable contribution to the intensity at a more or less high temperature. This outlines the necessity of performing a calculation which includes these possibilities. For the two phonon processes the diagrams of higher order in the perturbation expansion yield the most important contribution. In this way, diagrams of low order in many phonon exchange could be perharps neglected.

References

[1] ARMAND, G. and MANSON, J. R., *Phys. Rev. Lett.* 53 (1984) 1112.

[2] ARMAND, G. and MANSON, J. R., *Dynamics on Surfaces* 17 (1984) 59 (D. Reidel publishing company).

[3] JAYANTHI, C. S., ARMAND, G. and MANSON, J. R., *Surf. Sci. Lett.* 154 (1985) L247.

[4] LEVI, A. C. and SUHL, H., *Surf. Sci.* 88 (1979) 221.

[5] ESBJERG, N. and NORSKOV, J. K., *Phys. Rev. Lett.* 45 (1980) 807.

[6] ARMAND, G., *J. Physique* 38 (1977) 989.

[7] JAYANTHI, C. S., TOSATTI, E. and FASOLINO, A., *Phys. Rev.* B 31 (1985) 470.

[8] NICKLOW, R. M., GILAT, G., SMITH, H. G., RAUBENHEIMER, L. J. and WILKINSON, M. K., *Phys. Rev.* 164 (1967) 922.

[9] NILSSON, G. and ROLANDSON, S., *Phys. Rev.* B 7 (1973) 2393.

[10] MILLER, A. P. and BROCKHOUSE, B. N., *Can. J. Phys.* 49 (1971) 704.

[11] GORSE, D., SALANON, B., FABRE, F., KARA, A., PERREAU, J., ARMAND, G., LAPUJOULADE, J., *Surf. Sci.* 147 (1984) 611.

[12] LAPUJOULADE, J. and PERREAU, J., *Phys. Scripta* T 4 (1983) 138.

[13] SALANON, B., *J. Physique* 45 (1984) 1373.

[14] LAPUJOULADE, J., LE CRUER, Y., LEFORT, M., LEGAY, Y. and MAUREL, E., *Surf. Sci.* 103 (1981) L85.

[15] LAPUJOULADE, J., LEJAY, Y. and ARMAND, G., *Surf. Sci.* 95 (1980) 107.

[16] GORSE, D. and LAPUJOULADE, J., *Surf. Sci.* 162 (1985) 847.

[17] PERREAU, J., LAPUJOULADE, J., *Surf. Sci.* 122 (1982) 341.